JACS
JOURNAL OF THE AMERICAN CHEMICAL SOCIETY
Article
pubs.acs.org/JACS

Oxyanion Steering and CH−π Interactions as Key Elements in an N-Heterocyclic Carbene-Catalyzed [4 + 2] Cycloaddition

Scott E. Allen,[†] Jessada Mahatthananchai,[‡] Jeffrey W. Bode,*[,‡] and Marisa C. Kozlowski*[,†]

[†]Department of Chemistry, Roy and Diana Vagelos Laboratories, University of Pennsylvania, Philadelphia, Pennsylvania 19104, United States

[‡]Laboratorium für Organische Chemie, ETH-Zürich, Zürich 8093, Switzerland

Supporting Information

ABSTRACT: The N-heterocyclic carbene catalyzed [4 + 2] cycloaddition has been shown to give γ,δ-unsaturated δ-lactones in excellent enantio- and diastereoselectivity. However, preliminary computational studies of the geometry of the intermediate enolate rendered ambiguous both the origins of selectivity and the reaction pathway. Here, we show that a concerted, but highly asynchronous, Diels−Alder reaction occurs rather than the stepwise Michael-type or Claisen-type pathways. In addition, two crucial interactions are identified that enable high selectivity: an oxyanion-steering mechanism and a CH−π interaction. The calculations accurately predict the enantioselectivity of a number of N-heterocyclic carbene catalysts in the hetero-Diels−Alder reaction.

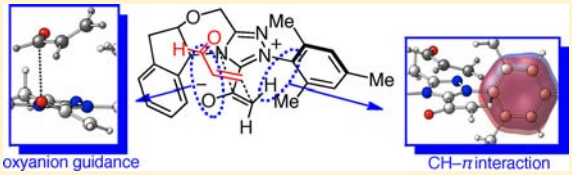

INTRODUCTION

N-Heterocyclic carbenes (NHCs) are effective in a large number of organocatalytic[1] and organometallic[2] applications. Starting in 2006, Bode and co-workers reported an NHC-catalyzed [4 + 2] cycloaddition between an enolate derived from α,β-unsaturated aldehydes or α-functionalized aldehydes and an enone as the diene.[3,4] These reactions displayed remarkable diastereo- and enantioselectivity, producing γ,δ-unsaturated δ-lactones in up to 99% ee and greater than 20:1 dr, as well as near-quantitative yields (eq 1).[5] Here, we establish

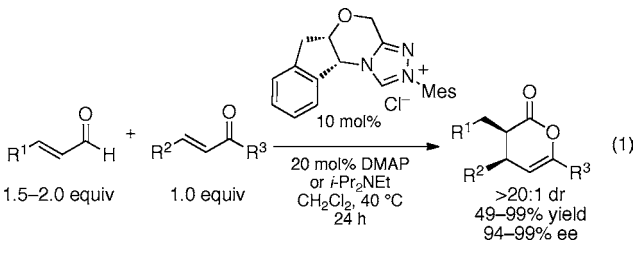

by computation that a concerted, but highly asynchronous, Diels−Alder reaction occurs rather than the stepwise Michael-type or Claisen-type pathways. Two crucial interactions were discovered that enable the high selectivity: an oxyanion-steering mechanism and a CH−π interaction. The calculations described herein accurately predicted the selectivity of a number of NHC catalysts in the hetero-Diels−Alder reaction.

The transformation in eq 1 is intriguing because the homoenolate equivalent (conjugated Breslow intermediate, **II**) undergoes proton transfer[6] to form an enolate intermediate (Scheme 1).[3,7] Alternatively, the enolate intermediate can also be reached from NHC attack on an α-chloroaldehyde[7] to obtain adduct **V**, followed by elimination of HCl. Unexpectedly,

Scheme 1. Proposed Catalytic Cycle for the NHC-Catalyzed Hetero-Diels−Alder Reaction (Only the NHC Core Shown)

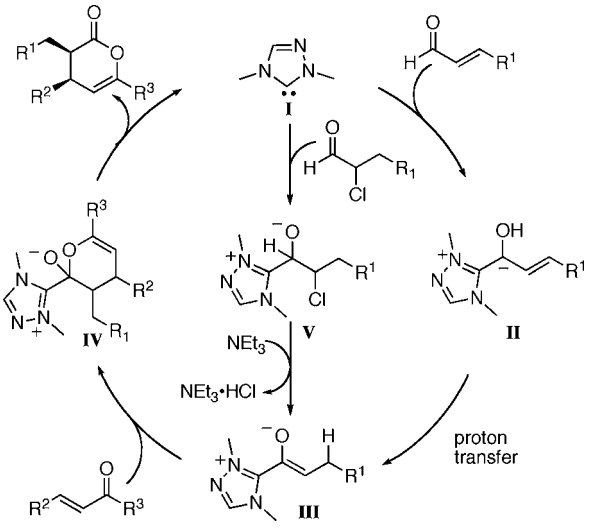

initial calculations showed that the enolate of **III** lies perpendicular to the triazolium and is not stabilized by conjugation with the NHC.[3b] Since the enolate is blocked by the indane on one side and mesitylene on the other, the origin of the high stereochemical fidelity was ambiguous.

METHODS

All calculations were performed using Gaussian 09.[8] All transition states were optimized with HF/6-31G(d) in the gas phase and were

Received: March 21, 2012
Published: July 4, 2012

   dx.doi.org/10.1021/ja302761d | J. Am. Chem. Soc. 2012, 134, 12098−12103

confirmed to have one imaginary frequency; all local minima were optimized with HF/6-31G(d) and were found to have no imaginary frequencies. Intrinsic reaction coordinate calculations were performed regularly to confirm that the calculated transition states reflected the correct reaction. Gibbs Free Energies were calculated at 1 atm and 298.15 K and are uncorrected.[9]

Solvation with toluene was examined for the mesitylene, *para*-trifluoromethyl, and pentafluoro catalysts in the deprotonated Diels–Alder reaction using IEFPCM(toluene)-HF/6-31G(d)//HF/6-31G(d).

A solution of 2-chloro-3-phenylpropanal (26.0 mg, 0.15 mmol, 1.5 equiv), triethylamine (20.0 μL, 0.15 mmol, 1.5 equiv), and (*E*)-methyl 4-oxo-4-phenylbut-2-enoate (20.0 mg, 0.1 mmol, 1.0 equiv) was prepared using 0.5 mL of $PhCH_3$. This solution was transferred to a vial containing a chiral triazolium salt. The reactions were carried out at room temperature, and the products were isolated by preparative TLC using 7:1 hexanes/EtOAc. The identity of the product was confirmed by ^{1}H NMR, ^{13}C NMR, GC/MS, and LC/MS.[10] Percent conversion was determined by the integration of the product at 5.82–5.79 ppm against the enone starting material at 6.91–6.86 ppm. Percent enantiomeric excess was determined by SFC (AD-H, gradient 5–50% CO_2/*i*PrOH, t_r = 8.31 and 9.61 min). The absolute configuration was assigned based on the previous literature report.

RESULTS AND DISCUSSION

To understand the stereochemical factors in this system, we examined a model system with acetaldehyde enolate as the dienophile and acrolein as the diene (R^1 = R^2 = R^3 = H, eq 1 and Scheme 1) using HF/6-31G(d) in the gas phase. The entire NHC catalyst from eq 1 was employed to accurately determine its role.[11,12]

Analysis of the enantioselectivity determining step revealed three distinct plausible reaction pathways (Figure 1): (1) a concerted Diels–Alder reaction, (2) a Michael-type addition of the NHC-enolate to the enone followed by addition/elimination of the enolate intermediate to cyclize the ring and expel the NHC catalyst, or (3) an initial addition of the NHC-enolate to the enone carbonyl followed by Claisen rearrangement and collapse of the intermediate following the same pathway as the Michael-type reaction. Examination of options 1 and 2 rapidly revealed that the charge separation induced in the initial Michael-type reaction gave rise to much higher energy transition states relative to the Diels–Alder reaction.

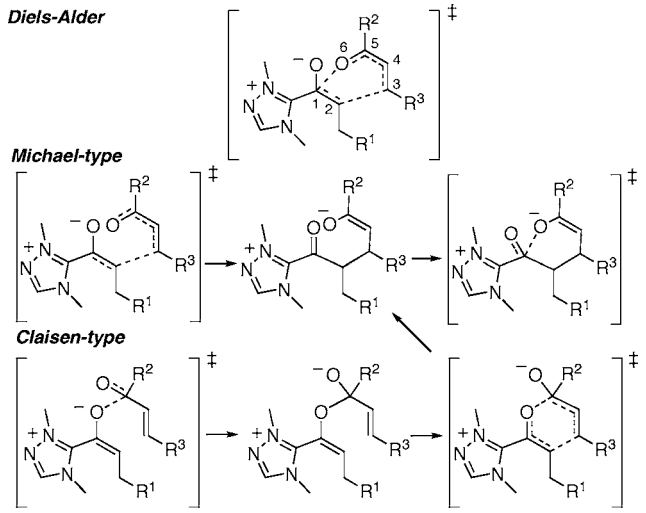

Figure 1. Possible reaction pathways.

For the Diels–Alder pathway, three constraints were identified: (1) the acrolein adopts a cisoid geometry to avoid undesirable charge separation in the transition state; (2) the acrolein does not approach endo to the triazolium, which creates prohibitive steric interactions between the diene and the mesitylene ring and gives rise to the incorrect diastereomer; and (3) the enolate substituent (R^1, Figure 1) is cis to the enolate oxygen to avoid steric interactions with the catalyst and to give rise to the correct diastereomer. Upon examination of conformations and optimization, transition states were located for the Diels–Alder pathway in which the enolates adopt a planar conformation with respect to the triazolium ring, a significant departure compared to the ground state enolates,[3c] which are perpendicular to the plane of the triazolium. This planarization of the enolate increases the positive charge on the enolate C1-carbon (Figure 1, top, and Figure 2, bottom) thereby optimizing the developing interaction with the negative charge on the diene oxygen.

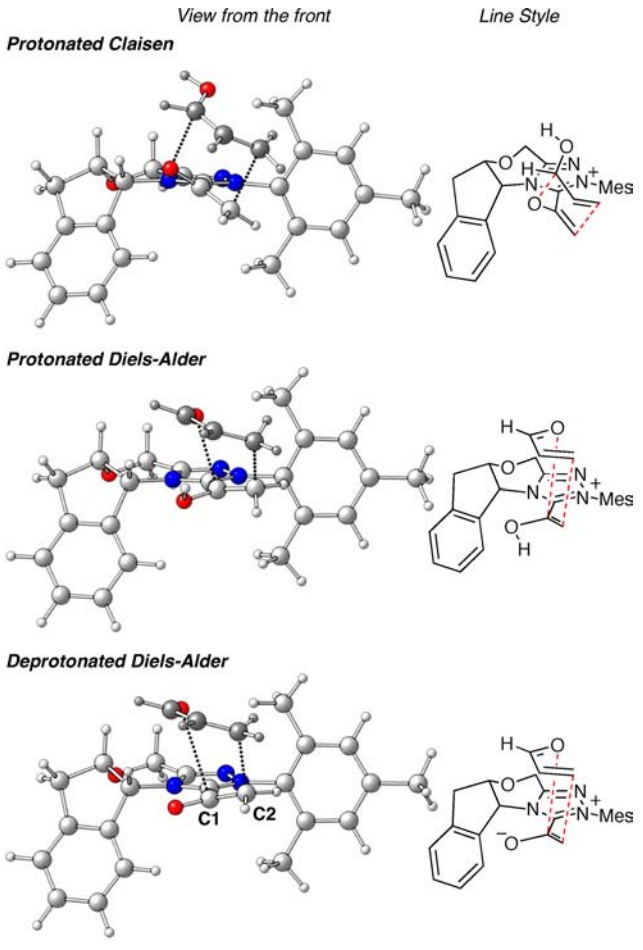

Figure 2. Sample Diels–Alder and Claisen transition states (one Claisen protonated, one DA protonated, and one zwitterionic DA) leading to the dihydropyranone products.

The transition state geometries indicate a very asynchronous Diels–Alder reaction. In the lowest energy model system transition state, the forming carbon–carbon bond is 2.109 Å while the forming carbon–oxygen bond is 3.049 Å. The atom–atom net linear natural localized molecular orbital natural population analysis (NLMO/NPA)[13] bond orders[14] are 0.435

dx.doi.org/10.1021/ja302761d | J. Am. Chem. Soc. 2012, 134, 12098–12103

and 0.0550 respectively. Similar values were seen for all the Diels–Alder transition states.[9]

Intrinsic reaction coordinate (IRC) calculations show that the enolate commences nearly perpendicular to the triazolium ring and flattens as the enone approaches. Notably, the starting geometry with the enolate oxygen up always leads to enone approach from the top face; the starting geometry with the enolate oxygen down always leads to enone approach from the bottom face (seen in IRCs of all the seven transition states located; see Figure 4). This trend suggests a secondary orbital interaction between the enone carbonyl π^* and an enolate lone pair (Figure 3), which guides the enone in its approach and ultimately leads to the Diels–Alder reaction.

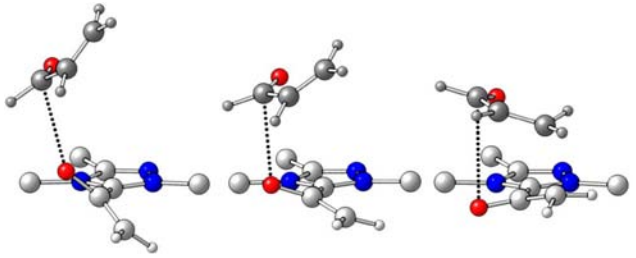

Figure 3. Oxyanion guiding interaction as seen in the intrinsic reaction coordinate calculation (NHC indane and mesitylene rings removed for clarity).

The presence of this interaction also suggests an alternative reaction pathway (Claisen-type, Figure 1) in which the enolate oxygen first adds to the enone carbonyl. Subsequent Claisen rearrangement of this intermediate would lead to the product.[15] When a protonated enolate was used in the calculation, this Claisen transition state was 8.5 kcal/mol lower in energy than the Diels–Alder reaction, but when the deprotonated enolate was used the model converged to the asynchronous Diels–Alder transition state. This suggests two possibilities: (1) if the reaction proceeds through the enolate, it possesses both Diels–Alder and Claisen character, and (2) if the complex reacts as the enol, it undergoes the Claisen rearrangement.[15a] The reaction is performed with catalytic DMAP or *i*-Pr_2NEt (water pK_a = 9.2 and 10.8, respectively), so the enol will dominate if its pK_a is above 12.

To calculate the pK_a values[16] of the relevant enolates, the method that Pulay[17] used with phenols was implemented except that the integral equation formalism variant of the polarization continuum model (IEFPCM) solvation method was employed instead of the COSMO model.[18] Each of the four enolate conformations was calculated, and the overall pK_a was generated from a weighted average of the four resultant values using a Boltzmann distribution at 25 °C. The resulting theoretical pK_a of the enolate in water is 5.5,[9] much less than that of the bases in water. Since the reactions under discussion here are conducted in toluene or dichloromethane, this estimate needs to be used with caution. However, analysis of the conjugate acids of other zwitterions, such as pyridine *N*-oxide, is informative. Here, the acid is a resonance-stabilized cation and the conjugate base is a zwitterion in which the negative charge is not stabilized by resonance. The pK_a of pyridine *N*-oxide is 0.79 in water and 1.63 in DMSO. On this basis we expect the pK_a of the triazolium enolate to be ~6.5 in DMSO (vs 9.00 for Et_3NH^+ in DMSO). Therefore, the main species in solution is most likely the enolate, for which the Claisen-type pathway does not occur.

In the Diels–Alder pathway there are the eight possible transition states differing by the ring conformation of the morpholine, the orientation of the enolate, and the facial approach of the enone. Upon examination of all the combinations, only seven of the eight transition states could be located (Figure 4); **TS5**, in which the morpholine oxygen orients cis to the indane, the enolate oxygen points toward the indane, and the acrolein approaches from the bottom, converged instead to **TS6**.

For the morpholine ring, interconversion between two different half-chair conformations causes a large distortion of the catalyst. When the morpholine oxygen orients down (cis to the indane), the indane ring extends in front of the triazolium alleviating steric interactions with the mesityl and resulting in the lowest energy conformation in the absence of enone. In this conformation, the indane more effectively blocks the approach of the substrate from the bottom face as seen in the energy difference of 6.65 kcal/mol between **TS3** and **TS7**, which vary only in the enone facial approach. In addition, this steric hindrance blocks enone approach in the counterpart of **TS1** (i.e., **TS5**) so effectively that it could not be located. In all cases where the enone approaches from the top, the lower energy conformation has the indane extended forward (**TS1** vs **TS2** and **TS3** vs **TS4**).

When the morpholine oxygen points up (trans to the indane), the indane ring tucks under the triazolium (e.g., **TS2**) incurring greater steric interactions with the mesityl as compared to the other half-chair conformation (cf. **TS1**). On the other hand, this conformation does open up approach from the bottom face of the enolate such that **TS6** is lower than **TS5** and **TS8** is lower than **TS7**. Even so, considerable steric blocking remains on the bottom face and all the transition states are higher in energy (**TS5**–**TS8**).

On the whole, the transition states with C2 of the enolate pointing toward the mesitylene are lower in energy than when it is pointing toward the indane due to a CH–π interaction between the terminal CH_2 of the enolate and the aromatic ring (Figure 5).[19−21] Specifically, the inner hydrogen on the enolate carbon is just 2.5 Å from C1 of the mesitylene, well within the combined van der Waals distance of 2.9 Å. Similar CH–π interactions have been observed in the transition states of Diels–Alder reactions,[22] sulfide oxidations,[23] and hydride reductions.[24] This effect can be increased with electron donating groups and diminished with withdrawing groups (see below).

To test the importance of the CH–π interaction, the eight transition states of the model system were optimized for a series of catalysts with varied aryl substitution and enantioselectivities were calculated using Boltzmann distributions (Table 1).[9,26] The calculations were performed concurrently with the reaction in eq 2. In principle, the stereoselectivity predictions provided are for both the α-haloaldehydes or the enals since they both yield the same enolate that precedes the stereoselectivity-determining step calculated here (Scheme 1). In practice, the enals are unreactive with catalysts lacking *ortho* substitution on the *N*-aryl ring due to reversibility in the formation of the initial adduct between the aldehyde and the NHC.[7]

Overall, the calculations were highly effective in anticipating the experimental selectivity, with the exception of entry 5. Further calculations revealed that M06-2X/6-311+G(d,p)[27]

dx.doi.org/10.1021/ja302761d | J. Am. Chem. Soc. 2012, 134, 12098–12103

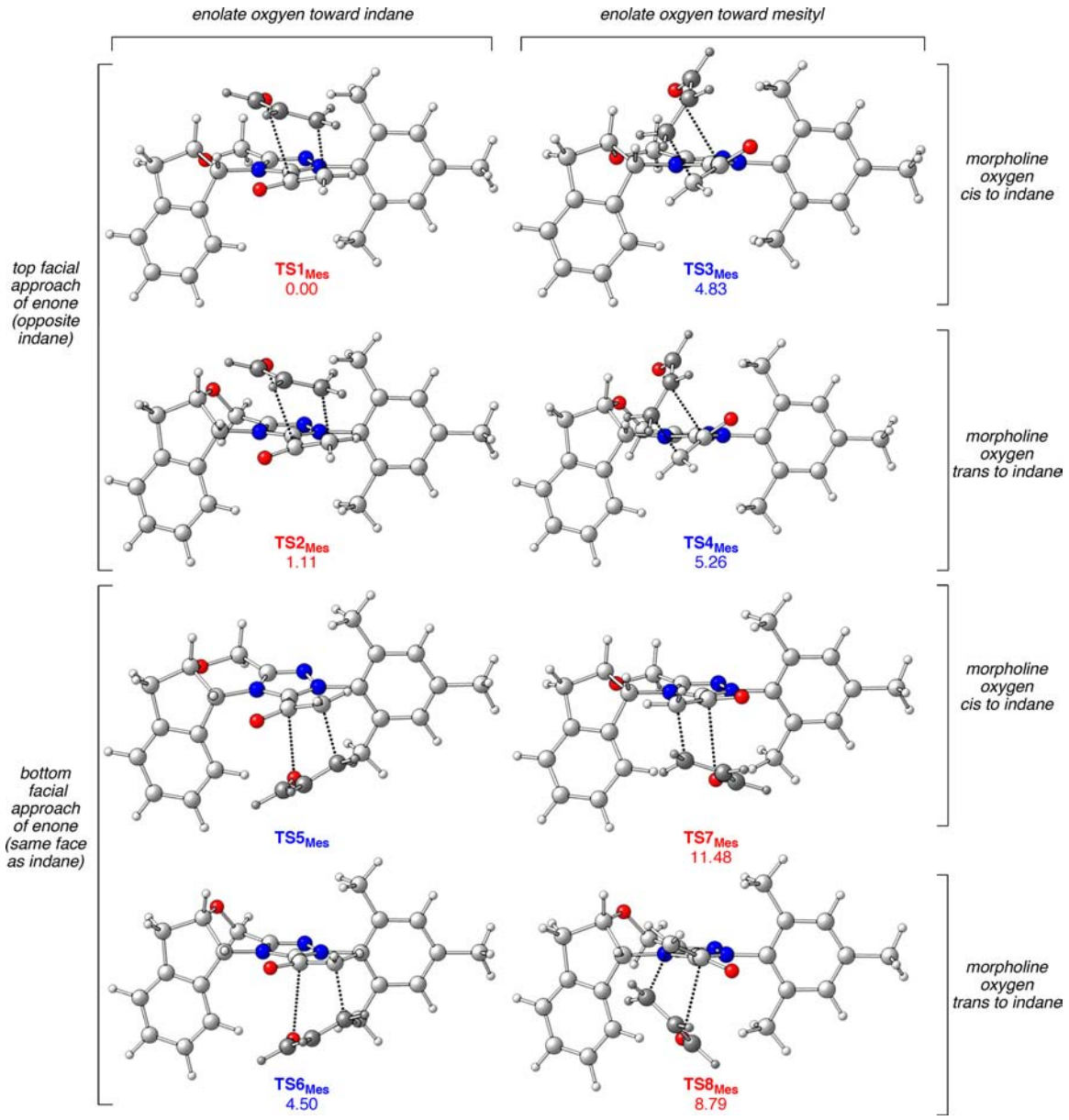

Figure 4. Eight possible transition states and relative free energies for the NHC-catalyzed Diels–Alder reaction (relative ΔG values in kcal/mol). Labels in red indicate transition states that lead to the major enantiomer; blue labels lead to the minor enantiomer.

single-point calculations of the full system were necessary to reproduce the experimental results in this case, which is attributed to the combination of five halogen substituents. Note that Table 1 contains all the catalysts that were examined computationally; none were excluded. Solvation with toluene was examined for the mesitylene, *para*-trifluoromethyl, and pentafluoro systems using IEFPCM(toluene)-HF/6-31G(d)//HF/6-31G(d) calculations of all the transition states; the computed selectivities did not change significantly, indicating that the gas phase calculations are sufficient for this reaction in this nonpolar solvent.[28]

A significant drop in selectivity was expected with electron-poor catalysts, which was confirmed in the experiments (entries 6–8). Analysis of the computational data shows that when Ar = mesitylene, the relative energy between **TS1** and **TS3**, which differ only in the orientation of the enolate, is 4.83 kcal/mol. When Ar = C_6F_5, that energy difference drops to 1.35 kcal/mol. The electron-poor arene cannot support the CH–π interaction, destabilizing **TS1**, **TS2**, **TS5**, and **TS6** relative to **TS3**, **TS4**, **TS6**, and **TS7**, and eroding the theoretical selectivity.

A Hammett analysis of the experimental results for aryls without *ortho*-substitution shows a strong correlation between the enantiomeric ratio and the electron density of the aryl ring ($\rho = -0.63$, $R^2 = 0.96$).[9] Electron-withdrawing groups attenuate the CH–π interaction, decreasing the enantiomeric ratio. On the other hand, *ortho*-substitution rescues even highly electron deficient catalysts (entries 4–5). Apparently, decreased rotational freedom of the *N*-aryl bond is a key factor in these transformations and a further analysis of this contribution is underway.

■ CONCLUSIONS

In summary, a computational model has been developed that successfully estimates the enantioselectivity of various catalysts in the NHC-catalyzed hetero-Diels–Alder reaction. Two effects account for the selectivity in these reactions: an oxyanion

dx.doi.org/10.1021/ja302761d | J. Am. Chem. Soc. 2012, 134, 12098–12103

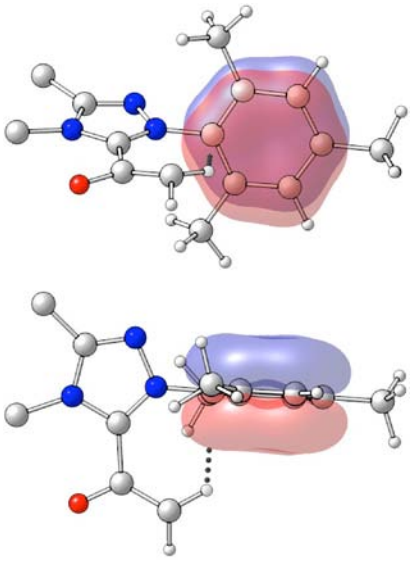

Figure 5. CH−π interaction from the front (top) and from overhead (bottom) for **TS1**. Enone and indane ring removed for clarity.

Table 1. Prediction of Reaction Selectivities Using the Computational Model

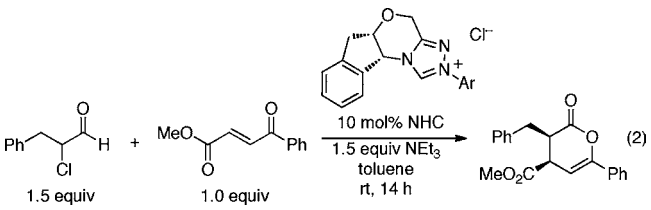

entry	aryl	calcd ee (%)[a]	conversion (%)	exptl ee (%)[b]
1	2,4,6-$(CH_3)_3$-C_6H_2	99.8 (100)	100	99
2	2-Me-4-OMe-C_6H_3	96.4	100	99
3	2-Me-C_6H_4	97.7	100	98
4	2,4,6-Cl_3-C_6H_2	97.3	95	99
5	2,4,6-Cl_3-C_6F_2	86.2 (99.6)	93	97
6	C_6F_5	81.5 (83.2)	47	76
7	3,5-$(CF_3)_2$-C_6H_3	84.1	34	89
8	4-CF_3-C_6H_4	87.5	15	95
9	C_6H_5	93.0	50	97
10	4-OMe-C_6H_4	95.0	75	98

[a]Calculated ee values for $R^1 = R^2 = R^3 = H$, eq 1 using HF/6-31G(d). Parenthetical amounts are for the full system (eq 2) at M06-2X/6-311+G(d,p)//HF/6-31G(d).[25] [b]Experimental ee values for the reaction in eq 2.

guiding interaction, which delivers the substrate, and a CH−π interaction. This study provides a basis for using these two elements in future development of catalyst systems.

■ ASSOCIATED CONTENT

Supporting Information

Full computational and experimental details and full citation of ref 8. This material is available free of charge via the Internet at http://pubs.acs.org.

■ AUTHOR INFORMATION

Corresponding Author

marisa@sas.upenn.edu; bode@org.chem.ethz.ch

Notes

The authors declare no competing financial interest.

■ ACKNOWLEDGMENTS

We are grateful to the National Institutes of Health (GM-079339 and GM-087605) and the National Science Foundation (CHE-0449587) for financial support of this research. Computing resources were provided by the National Science Foundation (CRIF CHE-0131132) and XSEDE (TG-CHE110080). We thank Bill Dailey for helpful discussions.

■ REFERENCES

(1) (a) Enders, D.; Niemeier, O.; Henseler, A. *Chem. Rev.* **2007**, *107*, 5606−5655. (b) Moore, J. L.; Rovis, T. *Top. Curr. Chem.* **2009**, *291*, 77−144. (c) Chiang, P.-C.; Bode, J. W. *N-Heterocyclic Carbenes*; The Royal Society of Chemistry: 2011; pp 399−435 (d) Nair, V.; Menon, R. S.; Biju, A. T.; Sinu, C. R.; Paul, R. R.; Jose, A.; Sreekumar, V. *Chem. Soc. Rev.* **2011**, *40*, 5336−5346. (e) Bugaut, X.; Glorius, F. *Chem. Soc. Rev.* **2012**, *41*, 3511−3522.

(2) (a) For a review of the application of NHC−Pd complexes, see: Kantchev, E. A. B.; O'Brien, C. J.; Organ, M. G. *Angew. Chem., Int. Ed.* **2007**, *46*, 2768−2813. (b) For other metals, see: Díez-González, S.; Marion, N.; Nolan, S. P. *Chem. Rev.* **2009**, *109*, 3612−3676.

(3) (a) He, M.; Struble, J. R.; Bode, J. W. *J. Am. Chem. Soc.* **2006**, *128*, 8148−8150. (b) He, M.; Uc, G. J.; Bode, J. W. *J. Am. Chem. Soc.* **2006**, *128*, 15088−15089. (c) Kaeobamrung, J.; Kozlowski, M. C.; Bode, J. W. *Proc. Natl. Acad. Sci. U.S.A.* **2010**, *107*, 20661−20665.

(4) For an intramolecular variant, see: Phillips, E. M.; Wadamoto, M.; Chan, A.; Scheidt, K. A. *Angew. Chem., Int. Ed.* **2007**, *46*, 3107−3110.

(5) For selected, related works from other groups, see: (a) Zhang, Y.-R.; Lv, H.; Zhou, D.; Ye, S. *Chem.—Eur. J.* **2008**, *14*, 8473−8476. (b) Kobayashi, S.; Kinoshita, T.; Uehara, H.; Sudo, T.; Ryu, I. *Org. Lett.* **2009**, *11*, 3934−3937. (c) Lv, H.; Mo, J.; Fang, X.; Chi, Y. R. *Org. Lett.* **2011**, *13*, 5366−5369.

(6) The mechanism of this proton transfer is explored in: (a) Verma, P.; Patni, P. A.; Sunoj, R. B. *J. Org. Chem.* **2011**, *76*, 5606−5613. (b) Reddi, Y.; Sunoj, R. B. *Org. Lett.* **2012**, *14*, 2810−2813.

(7) Mahatthananchai, J.; Bode, J. W. *Chem. Sci.* **2012**, *3*, 192−197.

(8) Frisch, M. J., et al. *Gaussian 09*, revision B.01; Gaussian, Inc.: Wallingford, CT, 2010.

(9) See Supporting Information for computational details.

(10) He, M.; Struble, J. R.; Bode, J. W. *J. Am. Chem. Soc.* **2006**, *128*, 15088−15089.

(11) Calculations of other NHC-catalyzed reactions with truncated catalysts: (a) Tang, K.; Wang, J.; Cheng, X.; Hou, Q.; Liu, Y. *Eur. J. Org. Chem.* **2010**, 6249−6255. (b) Zhao, L.; Chen, X. Y.; Ye, S.; Wang, Z.-X. *J. Org. Chem.* **2011**, *76*, 2733−2743. (c) Piel, I.; Steinmetz, M.; Hirano, K.; Fröhlich, R.; Grimme, S.; Glorius, F. *Angew. Chem., Int. Ed.* **2011**, *50*, 4983−4987. (d) Wei, S.; Wei, X.-G.; Su, X.; You, J.; Ren, Y. *Chem.—Eur. J.* **2011**, *17*, 5965−5971. (e) Verma, P.; Patni, P. A.; Sunoj, R. B. *J. Org. Chem.* **2011**, *76*, 5606−5613. (f) Hawkes, K. J.; Yates, B. F. *Eur. J. Org. Chem.* **2008**, 5563−5570.

(12) Calculations of other NHC-catalyzed reactions with full catalysts: (a) Dudding, T.; Houk, K. N. *Proc. Natl. Acad. Sci.* **2004**, *101*, 5770−5775. (b) Berkessel, A.; Elfert, S.; Etzenbach-Effers, K.; Teles, J. H. *Angew. Chem., Int. Ed.* **2010**, *49*, 7120−7124. (c) Wei, D.; Zhu, Y.; Zhang, C.; Sun, D.; Zhang, W.; Tang, M. *J. Mol. Catal. A.: Chem.* **2011**, *334*, 108−115. (d) Um, J. M.; DiRocco, D. A.; Noey, E. L.; Rovis, T.; Houk, K. N. *J. Am. Chem. Soc.* **2011**, *133*, 11249−11254. (e) Ryan, S. J.; Stasch, A.; Paddon-Row, M. N.; Lupton, D. W. *J. Org. Chem.* **2012**, *77*, 1113−1124. (f) DiRocco, D. A.; Noey, E. L.; Houk, K. N.; Rovis, T. *Angew. Chem., Int. Ed.* **2012**, *51*, 2391−2394.

(13) (a) Reed, A. E.; Curtiss, L. A.; Weinhold, F. *Chem. Rev.* **1988**, *88*, 899−926. (b) Reed, A. E.; Weinstock, R. B.; Weinhold, F. *J. Chem. Phys.* **1985**, *83*, 735−746. (c) Reed, A. E.; Weinhold, F. *J. Chem. Phys.* **1985**, *83*, 1736−1740.

(14) Glendening, E. D.; Reed, A. E.; Carpenter, J. E.; Weinhold, F. *NBO Version 3.1*.

(15) (a) Kaeobamrung, J.; Mahatthananchai, J.; Zheng, P.; Bode, J. W. *J. Am. Chem. Soc.* **2010**, *132*, 8810−8812. (b) Wanner, B.; Mahatthananchai, J.; Bode, J. W. *Org. Lett.* **2011**, *13*, 5378−5381.
(16) For a review: Alongi, K. S.; Shields, G. C. In *Annual Reports in Computational Chemistry*; Wheeler, R. A., Ed.; Elsevier; Vol. *6*, pp 113−138.
(17) (a) Zhang, S.; Baker, J.; Pulay, P. *J. Phys. Chem. A* **2010**, *114*, 425−431. (b) Zhang, S.; Baker, J.; Pulay, P. *J. Phys. Chem. A* **2010**, *114*, 432−442.
(18) For comparison of solvation models, see: Tomasi, J.; Mennucci, B.; Cammi, R. *Chem. Rev.* **2005**, *105*, 2999−3093.
(19) For reviews on the CH/π interaction: (a) Nishio, M.; Hirota, M.; Umezawa, Y. *The CH/π Interaction: Evidence, Nature, and Consequences*; Wiley-VCH: New York, NY, 1998. (b) Nishio, M. *Tetrahedron* **2005**, *61*, 6923−6950. (c) Nishio, M.; Umezawa, Y.; Honda, K.; Tsuboyama, S.; Suezawa, H. *CrystEngComm* **2009**, *11*, 1757−1788.
(20) For a review on the CH/π interaction in organic conformations, see: Takahashi, O.; Kohno, Y.; Nishio, M. *Chem. Rev.* **2010**, *110*, 6049−6076.
(21) After this manuscript was submitted, a report (ref 6b) appeared on calculations of NHC enolates reaching some similar conclusions.
(22) (a) Gordillo, R.; Houk, K. N. *J. Am. Chem. Soc.* **2006**, *128*, 3543−3553. (b) Anderson, C. D.; Dudding, T.; Gordillo, R.; Houk, K. N. *Org. Lett.* **2008**, *10*, 2749−2752.
(23) Capozzi, M. A. M.; Centrone, C.; Fracchiolla, G.; Naso, F.; Cardellicchio, C. *Eur. J. Org. Chem.* **2011**, 4327−4334.
(24) Gutierrez, O.; Iafe, R. G.; Houk, K. N. *Org. Lett.* **2009**, *11*, 4298−4301.
(25) Zhao, Y.; Truhlar, D. G. *Theor. Chem. Acc.* **2008**, *120*, 215−241.
(26) For a review on the electronics of NHC catalysts, see: Dröge, T.; Glorius, F. *Angew. Chem., Int. Ed.* **2010**, *49*, 6940−6952.
(27) This functional reduces inflated relative energies seen in HF: Simón, L.; Goodman, J. M. *Org. Biomol. Chem.* **2011**, *9*, 689−700.
(28) Enantioselectivities calculated using toluene solvation (IEFPCM(toluene)-HF/6-31G(d)//HF/6-31G(d)): 2,4,6-(CH_3)-C_6H_2, 99.8% ee; 4-CF_3-C_6H_4, 90.7% ee; C_6F_5, 86.9% ee.